An Induction Generator System Using RFNN

SHB IRRENA KARUMURI
Ph.DResearch Scholar
Department of Electrical & Electronics Engineering,
JNTU KUKATPALLY; A.P, India .

Dr. M.SUSHAMA
Professor& Head of the Department,
Department of Electrical and Electronics Engineering,
JNTU KUKATPALLY;A.P, India.

Abstract—A frequency controlled three-phase induction generator (IG) system using ac–dc power converter is developed in this study. First, the indirect field-oriented mechanism is designed for the control of the IG. A novel fuzzy modeling is developed to determine the flux control current and the maximum output power of the IG according to the rotor speed and the desired terminal voltage of the IG. Experimental results are provided to show the effectiveness of the proposed IG system using the RFNN controller for the dc-link power control. Finally, the control performance of the dc-link voltage control using the RFNN is also discussed.
Index Terms—induction generator (IG), recurrent fuzzy neural network (RFNN).

I.INTRODUCTION

In variable-speed wind turbine driven IG system, there is an appreciable amount of fluctuations in the magnitude and frequency of the generator terminal voltage due to varying rotor speed which is governed by the wind velocity and the pulsating input torque from the wind turbine and the load. This is objectionable to sensitive loads. In [1], system-identification experiments have been performed on a horizontal-axis wind turbine. In [2], a rule-based fuzzy logic controller to control the output power of a PWM inverter used in a stand-alone wind turbine driven IG system. Fuzzy-logic-based control is designed in [3] to optimize efficiency and enhance performance of wind generation system that uses a squirrel-cage IG and double-sided PWM converters. In [4], a sliding-mode control strategy is proposed to control the output power of IG and the stability at both minimum and no minimum operating regions are assured. The concept of incorporating fuzzy logic [5],[6] into a neural network has been grown into a popular research topic [7]–[9]. the fuzzy neural network (FNN) possesses both advantages; it combines the capability of fuzzy reasoning in handling uncertain information [5] and the capability of artificial neural networks in learning from processes [10], [11]. The recurrent fuzzy neural network (RFNN), which naturally involves dynamic elements in the form of feedback connections, used as internal memories the function of the network can be interpreted using fuzzy inference mechanism. The Electric frequency of the IG is controlled using the indirect field-oriented control mechanism. An online training RFNN with back propagation algorithm is introduced as the tracking controller for the dc-link power. The effectiveness of the RFNN controller, a linear integral–proportional(IP) [14] control is also adopted as the tracking controller of dc-link power for comparison. The more realistic way of control is to choose the dc-link voltage as the controlled variable. Therefore, a dc-link voltage control using the RFNN is also implemented the dynamic model of the indirect field-oriented control IG is derived. A novel fuzzy modeling for the rotor speed of the IG and the desired terminal voltage as the inputs, the flux control current and the maximum output power of the IG as the outputs is derived. Then, the tracking error of the dc-link power is regulated using a RFNN controller to result in the torque control current. A three-phase current controller under stationary reference frame is implemented to reduce the current harmonics and increase the power factor on the generator side to improve the efficiency of the generator. By using MATLAB software the frequency controlled IG system developed and simulated, and experimental results are given to verify the design of the proposed RFNN controlled IG system.

II. INDIRECT FIELD-ORIENTED CONTROLIGSYSTEM

The IG is controlled in a synchronously rotating reference frame with the *d*-axis oriented along the rotor-flux vector position decoupled control between the electromagnetic torque and the rotor excitation current is obtained. The machine model of an IG can be described in the synchronously rotating reference frame as follows:

$$V_{qs} = R_s i_{qs} + p\lambda_{qs} + \omega_e \lambda_{ds} \qquad (1)$$
$$V_{ds} = R_s i_{ds} + p\lambda_{ds} - \omega_e \lambda_{qs} \qquad (2)$$
$$V_{qr} = R_s i_{qr} + p\lambda_{qr} + (\omega_e - \omega_r)\lambda_{dr} \qquad (3)$$
$$V_{dr} = R_s i_{dr} + p\lambda_{dr} - (\omega_e - \omega_r)\lambda_{qr} \qquad (4)$$
$$T_e = \frac{3P}{4}\frac{L_m}{L_r}(i_{qs}\lambda_{dr} - i_{ds}\lambda_{qr}) \qquad (5)$$

Where p is the differential operator, V_{ds} and V_{qs} are the d,q axis stator voltages, V_{dr} and V_{qr} are the d,q axis rotor voltages,i_{ds} and i_{qs} are the d,q axis stator currents, R_s and R_r are the stator resistance and rotor resistance, ω_e and ω_r are the electricangular frequency and rotor angular speed, λ_{ds} and λ_{qs} are the d,q axis stator flux linkages, λ_{dr} and λ_{qr} are the d , q axis rotor flux linkages, P is the pole numbers, T_e is the electromagnetic torque, while L_m and L_r are the mutual inductance and rotorinductance, respectively.
The rotor currents can be represented using the rotor fluxes and stator currents as follows:

$$i_{qs} = \frac{1}{L_r}(\lambda_{qs}) - \frac{L_m}{L_r}(i_{qs}) \qquad (6)$$
$$i_{ds} = \frac{1}{L_r}(\lambda_{ds}) - \frac{L_m}{L_r}(i_{ds}) \qquad (7)$$

Substituting (6) and (7) into (3) and (4) yields

$$p\lambda_{qr} + \frac{R_r}{L_r}(\lambda_{qr}) - \frac{L_m}{L_r}R_r(i_{qs}) + (\omega_e - \omega_r)\lambda_{dr} = 0 \quad (8)$$
$$p\lambda_{dr} + \frac{R_r}{L_r}(\lambda_{dr}) - \frac{L_m}{L_r}R_r(i_{ds}) - (\omega_e - \omega_r)\lambda_{qr} = 0 \quad (9)$$

If the electric angular frequency in (8) is controlled in the following form:

$$\omega_e = \omega_r + \frac{L_m R_r i_{qs}}{L_r \lambda_{dr}} \qquad (10)$$

then, $\lambda_{qr} = exp^{\left(-\frac{R_r}{L_r}\right)}$ (11)

And $p\lambda_{dr} + \frac{R_r}{L_r}(\lambda_{dr}) - \frac{L_m}{L_r}R_r(i_{ds}) = 0$ (12)

Since all the motor parameters in (11) and (12) are positive, the stability of the system can be guaranteed. Consider the steady state condition; the following equations can be obtained:

$\lambda_{qr} = 0, p\lambda_{dr} = 0$ (13): $\lambda_{dr} = L_m i_{ds}$ (14)

Thus, the rotor flux in the d-axis can be controlled using i_{ds}. The torque (5) can be simplified to ,

$$T_e = \frac{3P}{4}\frac{L_m^2}{L_r}i_{ds}i_{qs} = K_t i_{qs} \qquad (15)$$

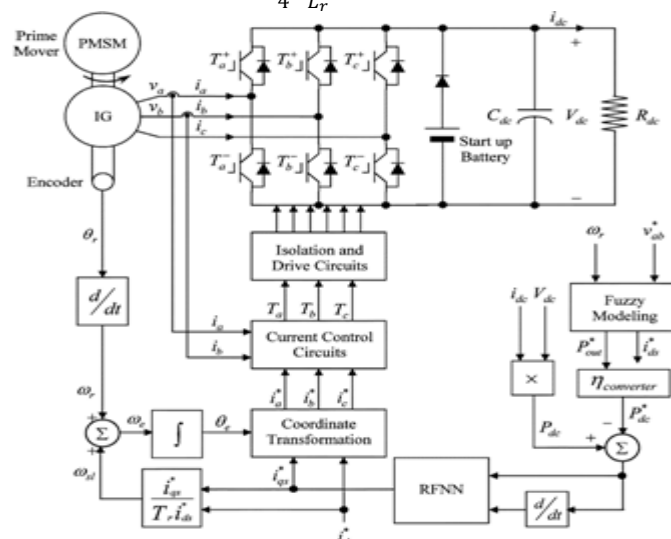Where, $K_t = \frac{3P}{4}\frac{L_m^2}{L_r}i_{ds}$, is a constant.

Fig 1: System configuration of frequency controlled IG system.

A permanent magnet synchronous motor (PMSM) directly coupled to the IG is adopted as the prime mover to simulate the operation of the wind turbine. The wind pattern could be easily programmed using the PMSM servo drive. The variable-frequency variable-voltage power generated by the IG is rectified to dc power by a PWM converter that also supplies lagging excitation current to the IG. The generator power is controlled using indirect field-oriented control with three-phase current control in the inner loops. The indirect field-oriented mechanism consists of a ramp comparison current-controlled PW Mac–dc power converter, a coordinate translator including a unit vector generator ,and a dc-link power control loop using RFNN. The machine flux is controlled in an open loop by control of the i_{ds} current. In nominal conditions, the rotor flux is set to the rated value for fast transient response. Moreover, a diode with a battery in the dc-link is used for the startup excitation of the IG. In Fig.1, θ_r is the position of the rotor; i_{ds}^* is the flux control current; i_{qs}^* is

the torque control current; θ_e is the electric angular angle; T_r is the time-constant of the rotor; ω_{sl} is the estimated slip speed; i_a^*, i_b^*, i_c^* are the three-phase command currents; v_a, v_b are the ab-phase voltages; i_a, i_b are the ab-phase currents; T_a, T_b, T_b are the PWM control signals i_{dc} is the dc-link current; V_{dc} is the dc-link voltage; P_{dc} is the dc-link power; P_{dc}^* is the command of the dc-link power; v_{ab}^* is the desired terminal voltage; P_{out}^* is the maximum output power of the IG; η is the efficiency of the PWM converter which is 90%. The IG used in this drive system is a three-phase connected four-pole 7.5-kW 120V/54 A2000 rpm type. The parameter soft he drive model at the nominal condition are R_s=0.17Ω, R_r=0.05Ω, L_s=0.0062 H, L_r=0.0064 H, L_m=0.0061 H (16)

The operating characteristics shown in Fig.2 are obtained using the current controlled in direct field-oriented IG system with constant load as shown in Fig.1.Though with the same flux control current in the IG threshold be an output voltage proportional to the rotor speed, the difference of output voltage at different rotor speeds is not obvious.
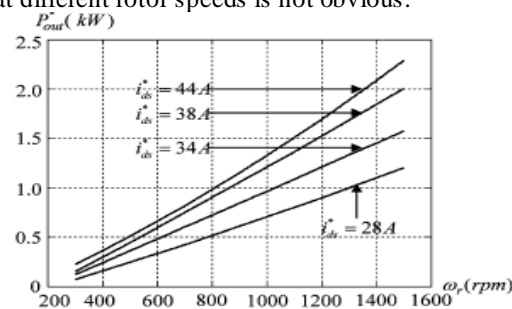

2(a) maximum-output-power to speed characteristic
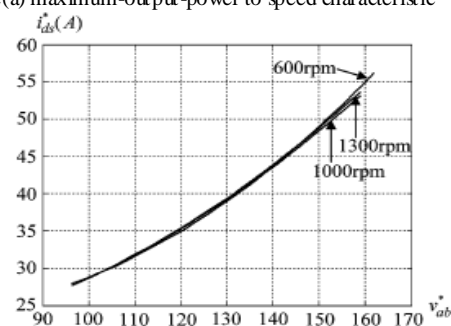
2(b)flux-control-current to terminal-voltage characteristic.

III. FUZZY MODELING

The variable-speed wind turbine driven IG systems are highly resonant, nonlinear and time-varying dynamics. Moreover, there is an appreciable amount of fluctuations in the magnitude and frequency of the generator terminal voltage due to varying rotor speed, which is governed by the wind velocity and the pulsating input torque from the wind turbine and the load. Therefore, a novel fuzzy modeling is developed to determine the flux control current and the maximum output power of the IG according to the rotor speed and desired terminal voltage of the IG using the knowledge embedded in the characteristic curves shown in Fig. 2(a) (b). According to the operating characteristics of the IG shown in Fig. 2(b), the characteristics of flux control

current to terminal voltage are seldom influenced by the Variations of the rotor speed under current controlled indirect field-oriented mechanism. Therefore, considering the possible parameter variations of the IG, a novel fuzzy control rule using the desired terminal voltage v_{ab}^* as the linguistic variable in the antecedent part and the flux control current i_{ds}^* as the variable in the consequent part is derived first. The proposed membership functions shown in Fig. 3(a) can be described by the following equations:

$$f_1: \quad m_1 = \begin{cases} 1, & 96 \leq v_{ab}^* < 110 \\ \frac{124 - v_{ab}^*}{124 - 110}, & 110 \leq v_{ab}^* < 124 \\ 0, & \text{otherwise} \end{cases} \quad (17)$$
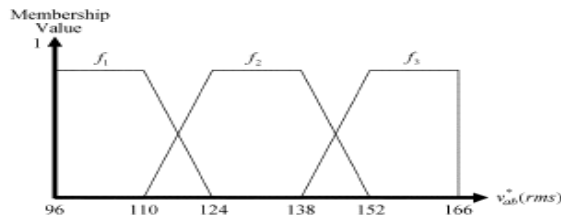
Fig 3 (a): Membership functions of desired terminal voltage v_{ab}^*

$$f_2: \quad m_2 = \begin{cases} \frac{110 - v_{ab}^*}{110 - 124}, & 110 \leq v_{ab}^* < 124 \\ 1, & 124 \leq v_{ab}^* < 138 \\ \frac{152 - v_{ab}^*}{152 - 138}, & 138 \leq v_{ab}^* < 152 \\ 0, & \text{otherwise} \end{cases} \quad (18)$$

$$f_3: \quad m_3 = \begin{cases} \frac{138 - v_{ab}^*}{138 - 152}, & 138 \leq v_{ab}^* < 152 \\ 1, & 152 \leq v_{ab}^* < 166 \\ 0, & \text{otherwise.} \end{cases} \quad (19)$$

Moreover, a novel defuzzification method is designed as follows to determine the flux control current:

$$y = \frac{\sum_{i=1}^{3} m_i f_i (v_{ab}^*)}{\sum_{i=1}^{3} m_i} = \sum_{i=1}^{3} m_i f_i (v_{ab}^*)$$
$$= m_1 f_1 (v_{ab}^*) + m_2 f_2 (v_{ab}^*) + m_3 f_3 (v_{ab}^*) = i_{ds}^*. \quad (20)$$

The linguistic values, membership functions, fuzzy control rules and de fuzzification of the proposed fuzzy modeling are chosen as follows:

Linguistic values:
Positive Big: PB, Negative Small: NS, Positive Medium: PM, Negative Medium: NM; Positive Small: PS, Negative Big: NB, Zero: ZE.

Membership Functions:
Depending on the special applications and the preference of the user, many types of membership functions can be selected. In this study, the triangle-shaped functions are chosen.Fig.3(b) is the membership functions for rotor speed ω_r;Fig.3(c) is the membership functions of flux control current i_{ds}^*;Fig.3(d) is the membership functions of the maximum output power of IG P_{out}^*.

TABLE 1 : LINGUISTIC RULE TABLE

i_{ds}^* \ ω_r	NB	NM	NS	ZE	PS	PM	PB
NB	NB	NB	NB	NM	NM	NM	NS
NM	NB	NB	NM	NM	NS	NS	NS
NS	NB	NM	NM	NM	NS	ZE	ZE
ZE	NB	NM	NS	NS	ZE	ZE	PS
PS	NB	NM	NS	NS	ZE	PS	PS
PM	NB	NM	NS	NS	ZE	PS	PM
PB	NM	NM	NS	ZE	PM	PM	PB
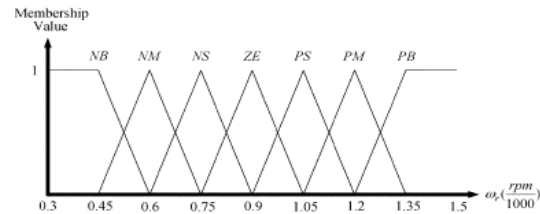
Fig 3 (b): Membership functions of rotor speed ω_r.
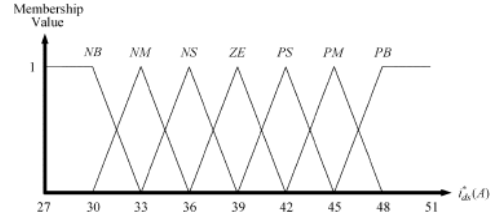
Fig 3 (c): Membership functions of rotor speed i_{ds}^*
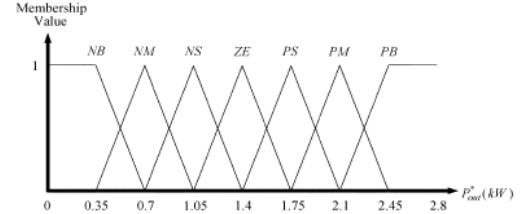
Fig 3 (d): Membership functions of rotor speed P_{out}^*

Construction of Fuzzy Rules
According to the operating characteristics shown in Fig.2(a), the linguistic rules for the fuzzy modeling of the IG, which are the "IF–THEN" forms, are formulated and listed in Table I. The rotor speed ω_r and the flux control current i_{ds}^* are the linguistic variables in the antecedent parts. The maximum output power of IG P_{out}^* is the linguistic variable.

De fuzzification:
The central of area (COA) method is implemented to result in the output.

IV. RECURRENT FUZZY NEURAL NETWORK

A four-layer RFNN as shown in Fig.4, which comprises the input (the I layer), membership (the j layer), rule (the k layer) and output layer (the o layer),is adopted to implement on line dc-link power control in this study. Moreover, $\bar{z}$

[1]represents a time delay and the output of the RFNN is recurrent to the input layer through a time delay.
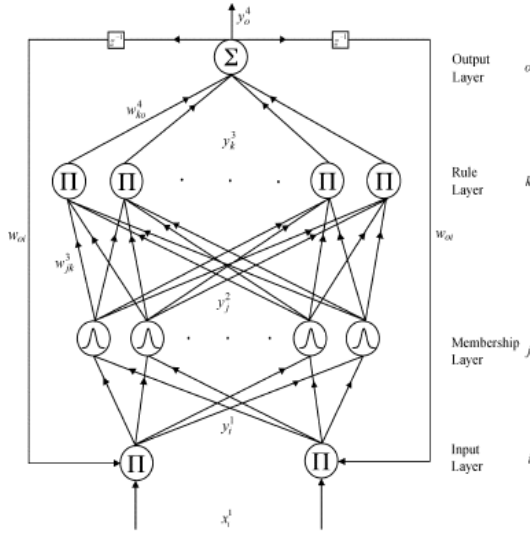

Fig. 4. Structure of four-layer RFNN.

The signal propagation and the basic function in each layer of the RFNN are introduced as follows:

Layer 1: input layer

Each node *I* in this layer is denoted by π, which multiplies the input signals and outputs the result of product. The net inputs and the net output are represented as

$$net_i^1(N) = \prod_o x_i^1(N) w_{oi} y_o^4(N-1)$$

$$y_i^1(N) = f_i^1\left(net_i^1(N)\right) = net_i^1(N), \quad i = 1, 2 \quad (21)$$

Where x_i^1 represent the inputs, $x_1^1 = P_{dc} - P_{dc}^* = e_m x_2^1 = pe_m$: N; denotes the number of iterations; ω_{oi} are the recurrent weights for the units in the output layer; y_4^0 is the output of the RFNN.

Layer 2: Membership Layer

In this layer, each node *j* in this layer performs a membership function. The Gaussian function is adopted as the membership function. For the *j*th node

$$net_j^2(N) = -\frac{(x_i^2 - m_{ij})^z}{(\sigma_{ij})^2}$$

$$y_j^2(N) = f_j^2\left(net_j^2(N)\right) = \exp\left(net_j^2(N)\right)$$

$$j = 1, \cdots, n \quad (22)$$

Where m_{ij} and σ_{ij} are, respectively, the mean and the standard deviation of the Gaussian function in the *j*th term of the *i*th input linguistic variable x_i^2 to the node of layer 2, and is the *n* total number of the linguistic variables with respect to the input nodes.

Layer 3: Rule Layer

Each node *k* in this layer is also denoted by π .For the *k*th rule node.

$$net_k^3(N) = \prod_j w_{jk}^3 x_j^3(N),$$

$$y_k^3(N) = f_k^3\left(net_k^3(N)\right) = net_k^3(N), \quad k = 1, \cdots, l \quad (23)$$

Where x_j^3 represents the *j*th input to the nodes of layer 3; ω_{jk}^3 the weights between the membership layer and the rule layer,

are designed to be unity; $l = (n/i)^i$ is the number of rules with complete rule connection if each input node has the same linguistic variables.

Layer 4: Output Layer

The single node *o* in this layer is labeled with ∑, which Computes the overall output as the summation of all input signals

$$net_o^4(N) = \sum_k w_{ko}^4 x_k^4(N)$$

$$y_o^4(N) = f_o^4\left(net_o^4(N)\right) = net_o^4(N), \quad o = 1 \quad (24)$$

Where the connecting weight w_{ko}^4 is the output action strength of the *o* the output associated with the *k*th rule x_k^4 represents the *k*th input to the nodes of layer 4; y_o^4 Is the control effort i_{qs}^*.

The online learning algorithms of the parameters w_{ko}^4, m_{ij}, σ_{ij} and ω_{oi} can be found in (22). To show the effectiveness of the RFNN with small rule set, the associated fuzzy sets with Gaussian function for each input signal are divided into N (negative), Z (zero), and P (positive) three membership functions. Therefore, nine linguistic rules are formed for two inputs. Moreover, the COA method is also used for defuzzification to result in one output. Thus, the RFNN has two, six, nine, and one neurons at the input, membership, rule and output layers, respectively. In addition, in order to obtain the best transient performance of the IG system, the learning-rate parameters of the RFNN are set to be

$$\eta_w = 2.05, \quad \eta_m = 0.111, \quad \eta_\sigma = 0.111, \quad \eta_r = 0.111. \quad (25)$$

V. DESIGN AND EXPERIMENTATION

The block diagram of the PC-DSP coprocessor control computer for the RFNN controlled IG system is shown in Fig.5. The fuzzy modeling and RFNN are realized in a PC. Two of the three-phase command currents i_a^* and i_b^* are sent to the power converter using digital/analog(D/A) converters. The current controlled PW Mac–dc power converter is implemented using IG BT switching components with a switching frequency of 15 kHz. In the main program, parameters and input/output (I/O) initialization are processed first. Then, the interrupt intervals for the ISRs are set. After enabling the interrupts, the main program is used to monitor control data. The ISR1 with 0.05ms sampling rate is the interface program between Pentium and DSP. The ISR1 first through D/A converters. The ISR2 with 2 ms sampling interval is used for reading the rotor position of the IG from encoder, executing the fuzzy modeling, reading dc-link voltage and current from analog/digital (A/D) converters, online training of the RFNN, executing the RFNN controller, and writing *d*-axis and *q*-axis command currents to the DPRAM. The subroutine in the DSP performs the integration of rotor flux angular speed and the coordinate transformation, and then writes the resulted three-phase command currents to the DPRAM.
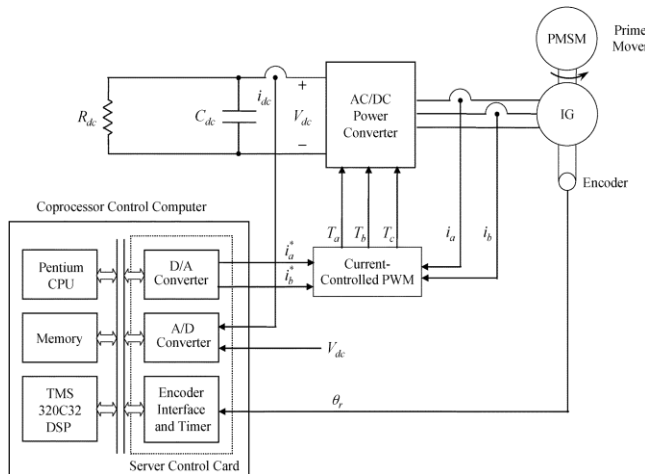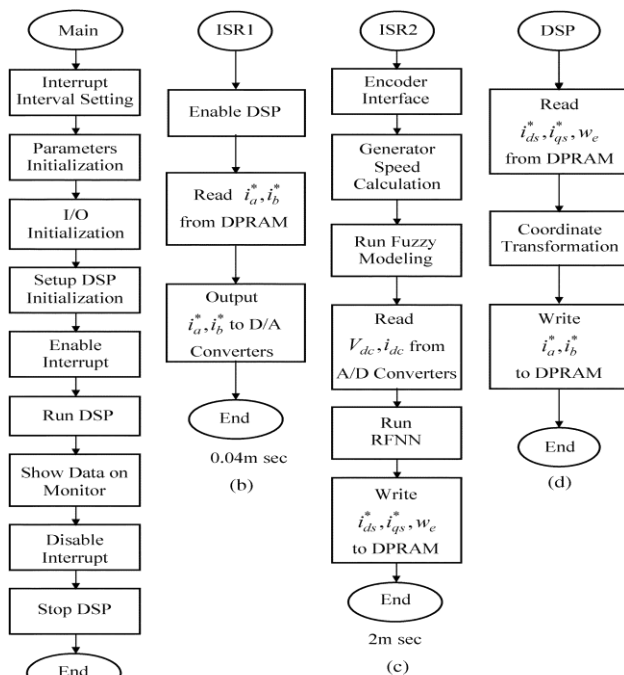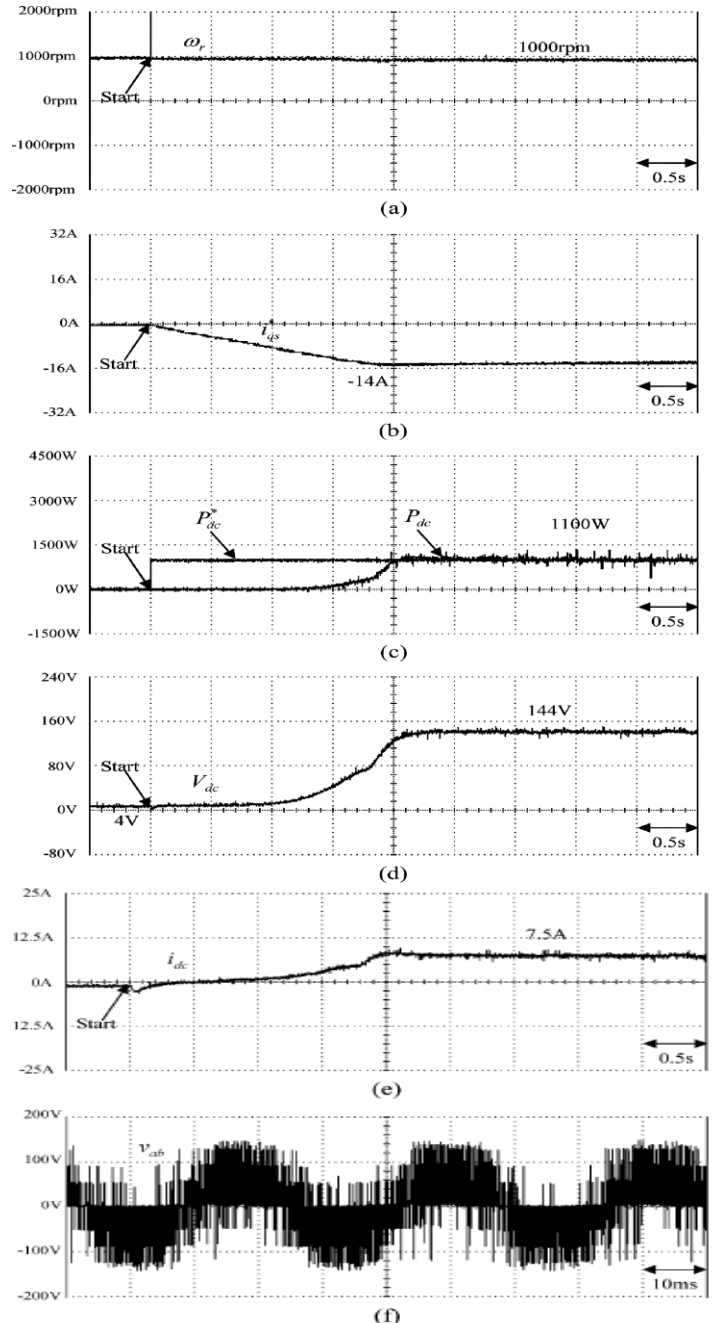
Fig.5. Coprocessor computer control IG system

Fig.6. Flowcharts of RFNN controlled IG system.

Fig. 7. (a)Experimental results of the IP dc-link power controlled IG system at 1000 rpm rotor speed ω_r (b) torque control current i^*_{qs}, (c) command P^*_{dc} and dc-link power P_{dc}. (d) dc-link voltage V_{dc}. (e) dc-linkcurrent i_{dc}.(f) terminal voltage v_{ab}.

First, operating conditions of the rotor speed, i.e., 1000 rpm, with the flux control current i^*_{ds} 38-A and 20-Ω loads are tested. First, the experimental results of the IP controlled IG system at 1000rpm due to the step command of P^*_{dc}, as shown in fig.7. Which is obtained from multiplying η of the converter with the output of the fuzzy modeling P^*_{out}, are discussed for the comparison of the control performance. Since the IG system is an online artime- varying system, the gains of the IP controller for the dc-link power tracking are obtained by try and error in order to achieve good transient and steady-state control performance at different operating conditions of the IG. The resulted gains are $K_P = 0.5$, $K_I =10$ at 1000rpm for the dc-link power tracking.

From the experimental results, sluggish dc-link power tracking are obtained for the IP controlled IG system due to the weak robustness of the linear controller.

The experimental results of the RFNN controlled IG system at 1000 rpm due to the step command of P^*_{dc} are shown in Fig.8.
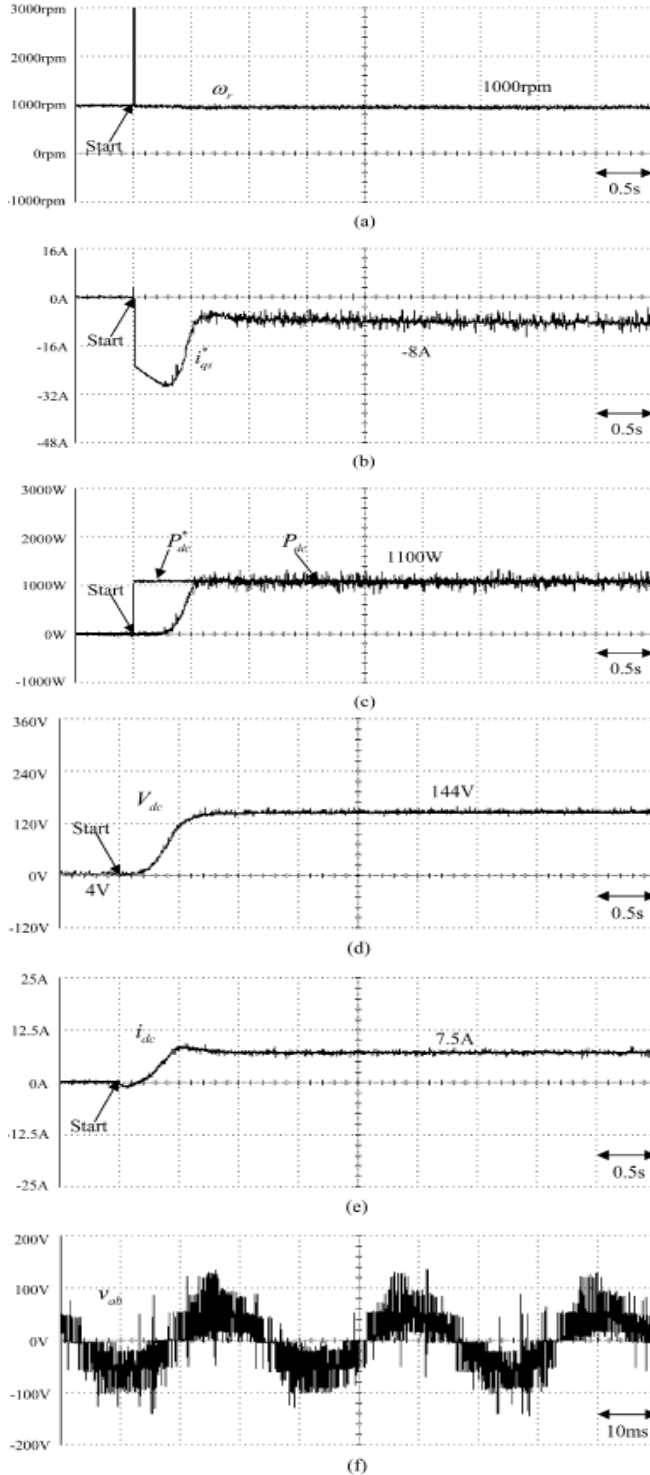
Fig. 8. (a)Experimental results of the RFNN dc-link power controlled IG system at 1000 rpm rotor speed ω_r (b) torque control current i^*_{qs}(c) command $P^*_{dc}$and dc-link power P_{dc} (d) dc-link voltage V_{dc}(e) dc-link current i_{dc}.(f) terminal voltage v_{ab}.

From the experimental results, excellent dc-link power tracking responses can be obtained for the RFNN controlled IG system owing to the online training of the RFNN.

Moreover, the robust control performance of the proposed RFNN controlled IG system at different operating conditions is excellent. Therefore, large torque control current is resulted only for the first 0.5s as shown in Fig.8(b). On the other hand, for the IP controlled IG system, large torque control currents$i^*_{qs}$are resulted as shown in Fig.7(b) due to the poor tracking control capability of the IP controller. However, large estimated slip speed ω_{sl} is also resulted for high torque control current. Thus, after the coordinate transformation, the resulted i^*_a of the IP controlled IG system is almost the same as the resulted i^*_a of the RFNN controlled IG system.

Next, some experimental results for the simulation of the Varying wind turbine speeds are provided. The experimental results of the RFNN controlled IG system at the condition of step changes of rotor speed, i.e., 550, 950, and 1200 rpm, for the command tracking of $P^*_{dc}$are shown in Fig.9.
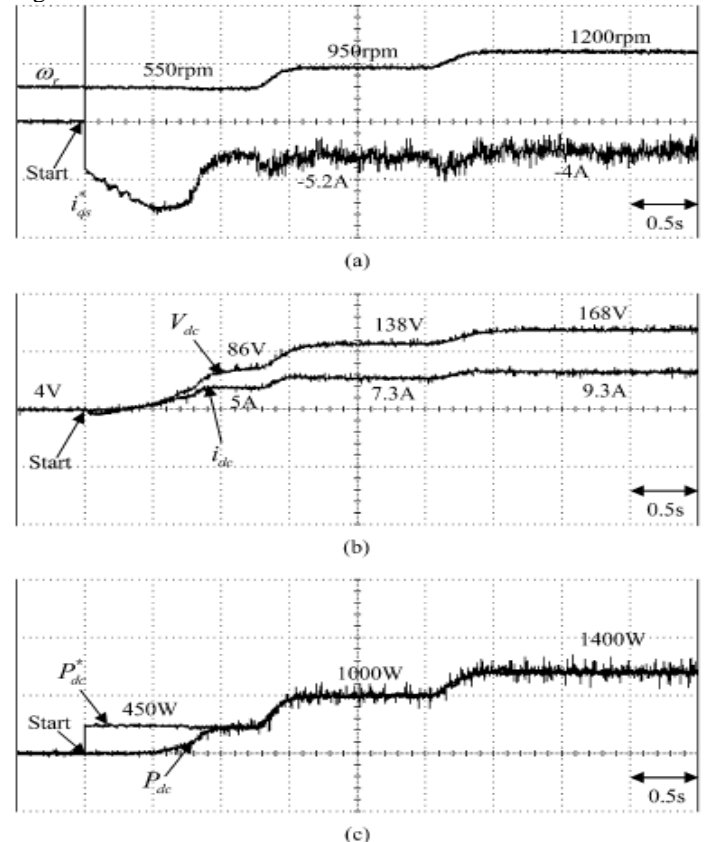

Fig.9. Experimental results of RFNN dc-link power controlled IG system at step-command changing of rotor speed: (a) rotor speed ω_r and torque control current i^*_{qs},(b) dc-link voltage V_{dc} and dc-link current i_{dc}, and (c) dc-link power command P^*_{dc} and dc-link power P_{dc}.

From the experimental results, the robustness of the RFNN controlled IG system is excellent for the continuous changing of operating condition.
Finally results of the RFNN controlled IG system for dc-link voltage control at 1000 rpm with 20Ω load and 33.33Ω load are shown in Figs. 10and 11, respectively.
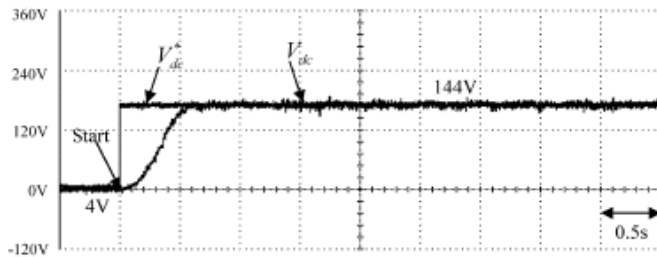
24

Fig.10. Experimental results of the RFNN dc-link voltage controlled IG systemat 20Ω load:dc-link voltage command V^*_{dc} and dc-link voltageV_{dc}
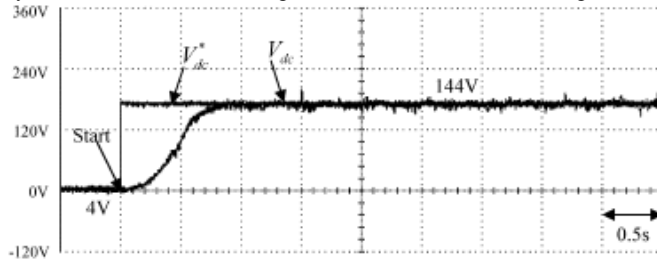

Fig.11. Experimental results of the RFNN dc-link voltage controlled IG system at 33.33Ω load dc-link voltage command V^*_{dc} and dc-link voltageV_{dc}

From the experimental results shown in Figs.10 and 11,favorable dc-link voltage control responses due to the step command of V^*_{dc} also can be achieved using the RFNN controller at various load conditions.

VI. CONCLUSION

Fuzzy modeling is proposed to obtain the desired flux control current and maximum output power of the IG at different operating conditions. A RFNN was proposed to control the dc-link power of the IG system at various rotor speeds. The RFNN was also proposed to control the dc-link voltage at various load conditions. The effectiveness of the proposed control scheme has been confirmed by some experimental results. In addition, the control performance of the proposed RFNN controlled IG system is robust with regard to parameter variations at different operating conditions of the IG.

REFERENCES

[1] P. Novak *et al.*, "Modeling and control of variable-speed wind-turbinedrive-system dynamics," *IEEE Contr. Syst. Mag.*, vol. 15, no. 4, pp.28–38, Aug. 1995.
[2] R. M. Hilloowala and A. M. Sharaf, "A rule-based fuzzy logic controllerfor a PWM inverter in a stand-alone wind energy conversion scheme," *IEEE Trans. Ind. Appl.*, vol. 31, no. 1, pp. 57–65, Jan./Feb. 1996.
[3] M. G. Simoes, B. K. Bose, and R. J. Spiegel, "Design and performanceevaluation of a fuzzy-logic-based variable-speed wind generationsystem," *IEEE Trans. Ind. Appl.*, vol. 33, no. 4, pp. 956–965,Jul./Aug. 1997.
[4] H. D. Battista, R. J. Mantz, and C. F. Christiansen, "Dynamical slidingmode power control of wind driven induction generators," *IEEE Trans.Energy Conv.*, vol. 15, no. 4, pp. 451–457, Dec. 2000.
[5] L. X. Wang, *A Course in Fuzzy Systems and Control*. Englewood Cliffs, NJ: Prentice-Hall, 1997.
[6] K. T. Tanaka and H. O.Wang, *Fuzzy Control Systems Design and Analysis*.New York: Wiley, 2001.
[7] F. J. Lin, R. J. Wai, and H. P. Chen, "A PM synchronous servo motordrive with an online trained fuzzy neural network controller," *IEEETrans. Energy Conv.*, vol. 13, no. 4, pp. 319–325, Dec. 1998.
[8] F. J. Lin, W. J. Hwang, and R. J.Wai, "A supervisory fuzzy neural networkcontrol system for tracking periodic inputs," *IEEE Trans. FuzzySyst.*, vol. 7, no. 1, pp. 41–52, Feb. 1999.
[9] Y. C. Chen and C. C. Teng, "A model reference control structure usinga fuzzy neural network," *Fuzzy Sets Syst.*, vol. 73, pp. 291–312, 1995.
[10] K. S. Narendra and K. Parthasarathy, "Identification and control ofdynamical systems using neural networks," *IEEE Trans. Neural Networks*,vol. 1, no. 1, pp. 4–27, Jan. 1990.
[11] Y. M. Park, M. S. Choi, and K. Y. Lee, "An optimal tracking neurocontrollerfor nonlinear dynamic systems," *IEEE Trans. Neural Networks*,vol. 7, no. 5, pp. 1099–1110, Sep. 1996.
[12] J. Zhang and A. J. Morris, "Recurrent neuro-fuzzy networks for nonlinearprocess modeling," *IEEE Trans. Neural Networks*, vol. 10, no. 2,pp. 313–326, Mar. 1999.
[13] F. J. Lin and C. H. Lin, "online gain-tuning IP controller using RFNN," *IEEE Trans. Aerosp. Electron. Syst.*, vol. 37, no. 2, pp. 655–670, Apr. 2001.
[14] F. J. Lin and R. J.Wai, "Hybrid controller using neural network for PM synchronous servo motor drive," *Proc. Inst. Elect. Eng.*, vol. 145, no. 3, pp. 223–230, 1998.